Molecular Crystals and Liquid Crystals Science and Technology. Section A. Molecular Crystals and Liquid Crystals

Publication details, including instructions for authors and subscription information:
http://www.tandfonline.com/loi/gmcl19

The Interaction of Light with Rb0.73Cr5Te8 and Polymer/Nanoferrite Composites

Charles J. O'connor [a] , Sichu Li [a] , Michel Evain [b] , James Gareth [b] & Vijay T. John [c]

[a] Department of Chemistry, University of New Orleans, New Orleans, Louisiana, 70148, USA

[b] Institute de Materieaux de Nantes, Nantes, France

[c] Department of Chemical Engineering, Tulane University, New Orleans, Louisiana, 70118, USA

Version of record first published: 04 Oct 2006

To cite this article: Charles J. O'connor, Sichu Li, Michel Evain, James Gareth & Vijay T. John (1997): The Interaction of Light with Rb0.73Cr5Te8 and Polymer/Nanoferrite Composites, Molecular Crystals and Liquid Crystals Science and Technology. Section A. Molecular Crystals and Liquid Crystals, 305:1, 095-108

To link to this article: http://dx.doi.org/10.1080/10587259708045049

Mol. Cryst. Liq. Cryst., 1997, Vol. 305, pp. 95–108
Reprints available directly from the publisher
Photocopying permitted by license only

THE INTERACTION OF LIGHT WITH $Rb_{0.73}Cr_5Te_8$ AND POLYMER/NANOFERRITE COMPOSITES

CHARLES J. O'CONNOR and SICHU LI,
Department of Chemistry, University of New Orleans,
New Orleans, Louisiana 70148 USA
MICHEL EVAIN and JAMES GARETH
Institute de Materieaux de Nantes, Nantes, France
VIJAY T. JOHN
Department of Chemical Engineering, Tulane University,
New Orleans, Louisiana, 70118 USA

Abstract The magnetic and photomagnetic characterizations of two materials are reported: ploymer/nanoferrite composites and the non-stoichiometric crystalline materials $Rb_{0.73}Cr_5Te_8$. In the inorganic-organic composite material, the inorganic component is iron oxide and the organic component is the polymer poly(p-ethylphenol) (PEP). The $Rb_{0.73}Cr_5Te_8$ material is a new non-stoichiometric formulation of the ACr_5Te_8 system that exhibits spin glass type magnetic behavior with a spin glass freezing temperature of 175K. The photomagnetism of both compounds has been measured at several temperatures below the spin blocking temperature.

INTRODUCTION

Photomagnetism is the change in the magnetic response of a material that results from exposure of that material to electromagnetic radiation.[1] The concept of the photomagnetic effect is often limited to those phenomena that have been observed through traditional magnetic detection methods (*i.e.*, magnetic susceptibility or magnetization measurements). The photomagnetic effect can arise from three basic routes. The first example of the photomagnetic effect is when a material absorbs radiation that results in the population of an excited state that has a different electronic configuration than the ground state. The duration of the magnetism that is induced in the material is therefore a measure of the lifetime of the state that is populated. A second example of Photomagnetism occurs when the absorption of radiation triggers a photochemical reaction that generates products with different magnetic properties than the reactants. The third example of a photomagnetic process involves a material that exhibits a hysteresis of its magnetic properties. The

electromagnetic radiation may result in the re-orientation of spins to a new configuration within the hysteresis of the material.

There have been several reports of each type of photomagnetism. A direct determination of the lifetime of the triplet state of the aromatic molecule coronene as well as the Curie-Weiss behavior of the paramagnetic phosphorescent triplet state of coronene have been reported from recordings of the magnetization as a function of time following single pulse excitation.[2] An interesting photomagnetic effect has been described by Gütlich and coworkers and has been termed light induced excited spin state trapping (LIESST).[3] These experiments describe the Photomagnetism that can be detected in some high-spin low-spin compounds. The use of spin crossover materials has been suggested by Kahn as a candidate for memory storage materials if the materials exhibit a suitable temperature dependent hysteresis of electronic states in the vicinity of room temperature.[4]

Photomagnetism from spin state conversion can also result from a photochemical reaction. Philo has reported magnetic studies of the flash photolysis of hemoglobin-carbon monoxide[5] using a SQUID magnetometer to monitor the reaction. The experimental decay of the paramagnetic signal was observed due to the pseudo-first order recombination of the Hb and CO (a large excess of CO is present).[5] Another recent report of a photomagnetic effect occurs in the photolysis of the cobalt-iron Prussian blue analog of the formula $K_{0.2}Co_{1.4}[Fe(CN)_6]\,6.9H_2O$.[6] Following irradiation of the sample with red light, a trapped metastable species is generated that exhibits enhanced magnetic response and hysteresis at low temperatures. Irradiation of the sample with blue light will partially diminish this photo-induced enhanced magnetic behavior. The material may be returned to its original magnetic configuration by heating the sample above 150K.

The physical properties of both superparamagnet and spin glass materials make them good candidates to exhibit photomagnetic effects. The photo-generation of magnetic bubbles in the amorphous intermetallic material Fe_2SnTe_4 has been observed.[7] Ferré and coworkers have also reported a related photomagnetic phenomenon that results from irradiation of frozen spin glasses consisting of metal doped aluminosilicate insulating spin glasses.[8] Those experiments involve a pulse of radiation that is delivered to the frozen spin glass and the subsequent magnetic response monitored with either Faraday rotation[8] or a SQUID susceptometer.[9] While Ferré's data suggest a possible electronic transition mechanism for destruction of the spin glass state, other reports of photomagnetic effects observed in spin glass systems deal primarily with radiational heating of the spin glass state resulting in a "melting" of the frozen spins.[10]

Due to the novel properties exhibited by particles of very small dimensions, there has been growing interest in the synthesis of nanoscale inorganic materials. Recently, many researchers have successfully synthesized fine particles exploiting the restricted environments offered by surfactant systems. Water-in-oil (w/o) microemulsions (also known as reversed micelles),[11] liquid crystals,[12] and vesicles[13] are examples of such systems used in nanoparticle synthesis. Here we describe the magnetic characterization and photomagnetic properties of an inorganic-organic composite material. The inorganic component is iron oxide and the organic component is the polymer poly(p-ethylphenol) (PEP).[14]

Another interesting compound arises from the family of materials AM_5X_8 (A = Li, Na, K, Rb, Cs, Cd, Sn, Pb, Ti; M = V, Cr, Ti; X = S, Se, Te) that have been reported to crystallize in the space group C2/m with the "Hollandite type" structure.[15] These materials contain M_5X_8 frameworks, consisting of layers of $CrTe_6$ octahedra, connected by double chains of edge sharing $CrTe_6$ octahedra, the coupling between the layers and the double chain being of the face sharing type. The secondary metal (*e.g.*, the alkali metal) resides in the resulting one dimensional channels. We report on the magnetic and photomagnetic effects of a new non-stoichiometric formulation $Rb_{0.73}Cr_5Te_8$[15] that is structurally related to this class of compounds and exhibits spin glass type magnetic behavior.

EXPERIMENTAL SECTION

Synthesis of $Rb_{0.73}Cr_5Te_8$

$Rb_{0.73}Cr_5Te_8$ was prepared from Rb (0.12g, 1.4 mmol), Cr (0.34g, 6.3 mmol), Te (1.28g, 10.0 mmol), sealed in a quartz tube under vacuum. The tube was heated to 650°C over a period of 6 hours, kept at 650°C for 2 days, then heated to 850°C over a period of 4 hours and subsequently, after 5 days, cooled to 400°C over a 60 hour period and continuously to room temperature for further 4 hours. A dark metallic-gray crystalline product was obtained from which layer single crystals of $Rb_{0.73}Cr_5Te_8$ were isolated.[15]

Synthesis of Ferrite Particles: Stock solutions of 0.5 M AOT [bis(2-ethylhexyl) sodium sulfosuccinate] were used in preparing the reversed micellar solutions containing the reactants $FeSO_4$ and NH_4OH. The so-called injection method was used in preparing all reversed micellar solutions. In a typical preparation, a predetermined amount of reactant stock solution was added to the AOT solution to yield the final reversed micellar solution with the required w/o ([H_2O:AOT] molar ratio of water to surfactant) and reactant concentration. The synthesis of ferrite particles was initiated by adding the NH_4OH reversed micellar solution to the $FeSO_4$ reversed micellar solution, while vigorously stirring the mixture. The solution instantly turned bluish-green and within minutes changed to a deep red color. The reaction mixture warm kept stirred for about 2 h.

Synthesis of Poly(p-ethylphenol) (PEP) Particles

The simplified mechanism of enzymatic polymerization is shown in Figure la. Phenoxy centers migrate to ortho positions where coupling occurs. The polymerization reaction is conducted in reversed micelles which solubilize the catalytic enzyme, horseradish peroxidase (HRP). Figure l b illustrates the structure of the twin-tailed anionic bis(2-ethylhexyl) sodium sulfosuccinate (AOT). Reversed micellar solutions of w/o (water to surfactant molar ratio) 10 were prepared using 0.01 M HEPES buffer at pH 7.5. As mentioned earlier, the particles are spherical and typically less than lμm in diameter. Both individual particles and clusters of spheres are observed.

Synthesis of the Ferrite-PEP Composite

After the synthesis of ferrite particles in reversed micelles, 3 ml aliquots were taken and oven-dried overnight at 40 'C to remove NH40H from the system. The dried material was then reconstituted to the same volume as the original aliquot by adding isooctane. The final solution is a clear deep-red solution containing ferrite particles sustained in a waterless microemulsion. To this solution, 2 ml of 0.5 M AOT/isooctane solution was added followed by the addition of 0.01 M HEPES buffer (pH 7.5), the monomer (EP), and the enzyme (HRP in buffer) to make up the final reaction mixture.

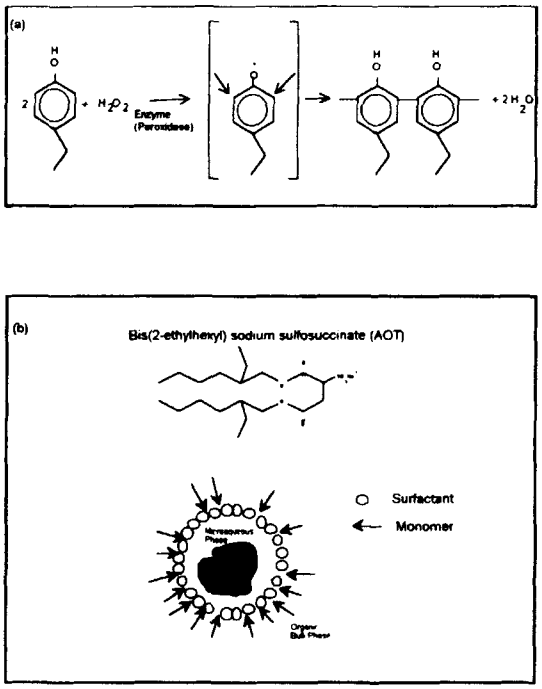

FIGURE 1 Simplified scheme for the enzyme catalyzed reverse micelle polymerization. (a)Phenoxy radical polymerization AOT (top) and (b)representation of the reverse micelle (bottom).

Magnetic Measurements

The magnetic properties of $Rb_{0.73}Cr_5Te_8$ and the ferrite-PEP composites were characterized using a Quantum Design, Inc. Model MPMS-5S superconducting (SQUID) susceptometer. Calibration and measurement procedures have been reported elsewhere.[16] Several experiments were conducted: magnetic susceptibility (χ_{dc}, MIH) as a function of temperature and magnetization as a function of field or temperature. Two different procedures were used for the de magnetic susceptibility experiments: (i) zero-field cooling, where the sample was slowly cooled in zero field to a temperature of 1.7 K at which the measuring field of 1.0 kG was switched on and

the magnetization was measured as a function of temperature, and (ii) field cooling where the field of 1.0 kG was turned on at a temperature well above the superparamagnetic or spin glass blocking temperature before the sample was cooled to 1.7 K.

For remanent magnetization measurement, both thermal remanent magnetization (TRM) and isothermal remanent magnetization (IRM) were obtained as a function of field and temperature. The TRM experiment involves slowly cooling the sample in an applied magnetic field to a measuring temperature below the blocking temperature and then switching off the field and measuring the remanent magnetization after a specified elapsed time of 300 s. On the other hand, IRM data are obtained by cooling the sample to the measurement temperature in zero field, applying a field for a long enough time (300 s) and then switching off the field and measuring the remanent magnetization after an elapsed time of 300 s. Standard M vs. H hysteresis loops were also recorded at different temperatures ranging from 2.0 to 300.0 K.

Photo-induced magnetic measurements

The photomagnetic data were recorded using an experimental technique based on the STEPS technique[2] that permits illumination of the sample with high intensity radiation while very precise magnetic data was being recorded on the SQUID susceptometer. The radiation was supplied by a high pressure xenon lamp and the duration of the pulse of radiation was determined with a mechanical shutter. A high optical purity quartz supracil light pipe with cross section area of 16mm^2 delivered the radiation to the specimen in the sample chamber of the superconducting susceptometer. In each case, approximately 100mg of sample was packed into a small quartz tube (5mm i.d.) that was attached to the end of the quartz light pipe. The photomagnetic response of the samples were measured at a variety of temperatures and at magnetic fields ranging from 1.0 to 5.0 kG following zero field cooling.

RESULTS AND DISCUSSION

Materials that exhibit highly frustrated magnetic exchange are good candidates for showing "spin glass" type magnetic behavior because they intrinsically posses order-disorder frustration in the orientations and interactions of the spins. The frustration arises in the two materials for different reasons. One material is a crystalline solid that nevertheless exhibits sufficient frustration to achieve a relatively high spin glass freezing temperature, and the other material consists of nanophase ferrite particles distributed in a uniform fashion in a polymeric matrix and exhibits superparamagnetism. The magnetic susceptibility data of both materials were measured over the 1.7K to 300K temperature region. The ferrite magnetic characterization and photomagnetic response of the nanoparticle composites will be discussed first followed by $Rb_{0.73}Cr_5Te_8$.

Reversed micelles are nanodroplets of water sustained in an organic phase by a surfactant, typically an anionic, bis(2-ethylhexyl) sodium sulfosuccinate, also referred to as AOT. The water pools of the micelles are capable of solubilizing biomolecules such as enzymes, which retain catalytic activity in what is essentially a minimal water environment.

A remarkable aspect of polymerization in this media is that the polymer formed precipitates out from solution with the morphology of interconnected, submicron-sized spheres. While the full explanation of morphology development is as yet unclear, we do have evidence that the micelles have a templating effect, to fold chains as they are formed to the resulting spheres. As a consequence of the observation of polymer precipitation in the form of interconnected spheres, the concept of preparing polymer-nanoparticle composites arose through the argument that the precipitating polymer may also entrap and pull down inorganic clusters present in the micelles. Polymer-nanoparticle composites are prepared by a two step approach. In the first step, the water pools of the micelles are used to synthesize inorganic compounds whose growth would be restricted to the manometer size range by the microstructure synthesis environment. In the second step, monomer (p-ethylphenol) and enzyme are added to the system, and polymerization is initiated.

Reversed micelles constitute a microreactor environment to synthesize inorganic particles restricted to the nanometer size range. As shown by Lopez-Quintela and Rivas,[17] ferrite particles synthesized in reversed micelles have sizes approaching the magnetic domain size. Such Particles exhibit superparamagnetic properties. Here we show that incorporation of these ferrite particles into the polymer microspheres confers superparamagnetic properties to the composite.

Magnetic Properties

To determine the magnetic properties of the ferrite-PEP composite material, a SQUID magnetometer was used. Field-dependent hysteresis loops were generated in the temperature range 2.0-300K. Typical trends exhibited by the ferrite-PEP composites are described through the hysteresis loops recorded at 100 and 4.5 K, shown in Figure 2 a & b, respectively. The magnetization vs. field data at 100K

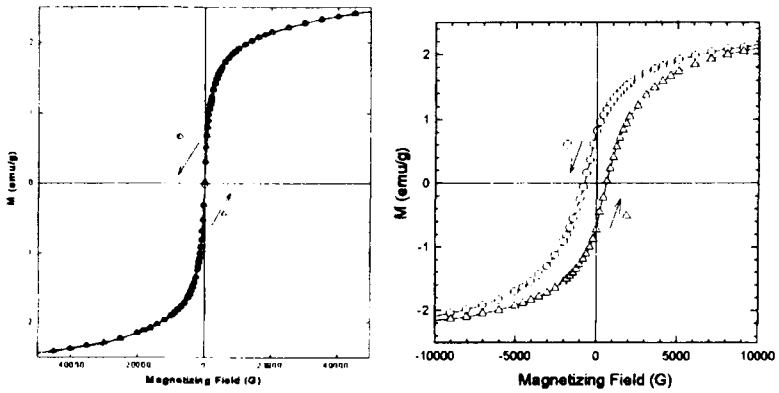

FIGURE 2 (a) Magnetic hysteresis loop for ferrite polymer composite at 100K. and (b) magnetic hysteresis loop at 4.5K.

illustrates that the data are perfectly superimposable as the field is cycled between ±50 kG, with the coercivity H=0. This lack of hysteresis is characteristic of superparamagnetic particles or some single-domain particles of very small dimensions. The particles have very small volumes, and thermal fluctuations are sufficient to

overcome the anisotropy energy barrier, allowing the magnetization to spontaneously reverse direction. As the temperature is significantly lowered to 4.5 K, the sample starts to display some hysteresis with coercivity H=700 G, as seen in Figure 2b. The presence of low-temperature hysteresis together with the absence of hysteresis at higher temperature confirms the superparamagnetism of the ferrite-PEP composite. If the sample did not show hysteresis at any temperature, it would be classified as being made of single-domain particles with the hard axis aligned.[18]

For superparamagnetic particles, the Langevin function[19] describes the relationship between the magnetization at a particular temperature (M_T) and the applied magnetic field (H) according to the expression shown below, where M_S is the saturation magnetization, μ is the magnetic moment of each particle, k is the Boltzmain constant, and T is the absolute temperature:

$$M_T = M_s\left[\coth\left(\frac{\mu H}{kT}\right) - \frac{kT}{\mu H}\right]$$

The above expression also describes paramagnetism, with μ representing the magnetic moment of a single atom. In the present case however, μ represents a single-domain particle comprised of $> 10^5$ atoms, which explains the term "superparamagnetism". As described in a recent paper by Yaacob and co-workers,[20] the slope of the magnetization curve near H = 0 can be used to estimate the size of the largest particles present in a sample of nonuniform particle sizes. Thus, the largest "magnetic" size of the particles can be related to parameters through the following expression:[20]

$$d_{mag(max)} = \left[\frac{18kT}{\pi} \times \frac{(dM \setminus dH)_{H=0}}{\rho M_S}\right]^{1/3}$$

where ρ is the density of maghemite (5.07 g/cm^3). In our calculations, the limiting slope near the origin was determined from the hysteresis plots by curve-fitting the linear portion of the data. The saturation magnetization for maghemite, M_S = 76.0 EMU/g, was also used in the calculations.[21] Estimates of $d_{mag(max)}$ show that the "magnetic" size increases as the w/o of the sample increases. The $d_{mag(max)}$ values illustrate a very small magnetic size (0.5-1.5 NM). From TEM measurements, clusters anywhere between 1 and 10 NM can be observed.[14] In general, the visually observed particle size is larger than the $d_{mag(max)}$ values; the disparity could perhaps be attributed to the magnetically 'dead" layer reported to be present on the surface of magnetic particles.[22] Better agreement may also be obtained by using the saturation magnetization (M_S) corresponding to the true ferrite phase composition rather than just using the M_S of maghemite. The XRD pattern indicates maghemite as the dominant phase, but because of the line broadening at these small particle sizes, the true phase composition is not easily estimated.

Temperature-dependent dc magnetic susceptibility data for the sample obtained by two different methods are shown in Figure 3. At high temperatures, the field-cooled (FC) and zero-field-cooled(ZFC) magnetization data exhibit the same trend.

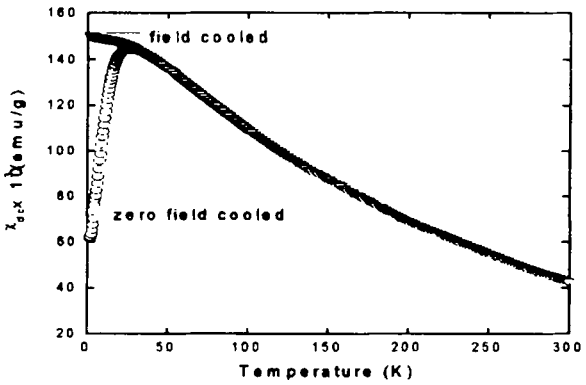

FIGURE 3 Field cooled (FC) and zero field cooled (ZFC) dc magnetic susceptibility data for the ferrite polymer composite plotted over the 1.7 to 300K temperature region.

However, at low temperatures they significantly diverge. The FC curve reaches a plateau and the ZFC curve shows a dramatic decrease in magnetization. From the ZFC data in Figure 3, it is apparent that there is a sharp maximum in the magnetization when plotted as a function of temperature. This maximum is a characteristic of spin glass type materials[23] and for the ferrite-PEP composite studied here, it occurs at 27.0 K. Magnetic particles of very small size are known to mimic some of the properties of spin glass materials and to exhibit blocking temperatures.[24] Going back to the hysteresis loops shown in Figure 2, it is worth noting that the sample exhibits hysteresis at temperatures below 27.0 K, with hysteresis vanishing at higher temperatures. The observation is consistent with the behavior of ultrafine magnetic particles.[25]

One of the frequently performed diagnostic experiments to characterize the spin glass state is the dependence of TRM and IRM on the applied magnetic field. The TRM and IRM data as a function of field at 4.5 K are shown in Figure 4. The TRM attains a maximum at 3 kG and then slowly decreases and remains essentially invariant above 20 kG. The IRM increases sharply till about 10 kG and eventually reaches a plateau at magnetic fields above 20 kG. The TRM and IRM curves converge at high magnetic fields indicating that the magnetic effects which lead to the blocking of particle moments are destroyed at these large fields. The magnitude of the TRM is always greater than the IRM due to the nature of the experiment. In the TRM experiment, the sample is slowly cooled in the presence of a magnetic field to a temperature below the blocking temperature, and then the field is switched off. The remanent magnetization is later measured after an elapsed time of 300 s. For the IRM experiment, the sample is first cooled below the blocking temperature in zero field, followed by exposure to magnetic field for a specified time of 300 s, turning off the field, and measuring the remanent magnetization after 300s. During the TRM experiment, the magnetic moments are frozen in partial alignment with the applied magnetic field when the temperature falls below the freezing temperature, causing the spin glass state. By switching off the field in the spin glass state, the magnetic field is

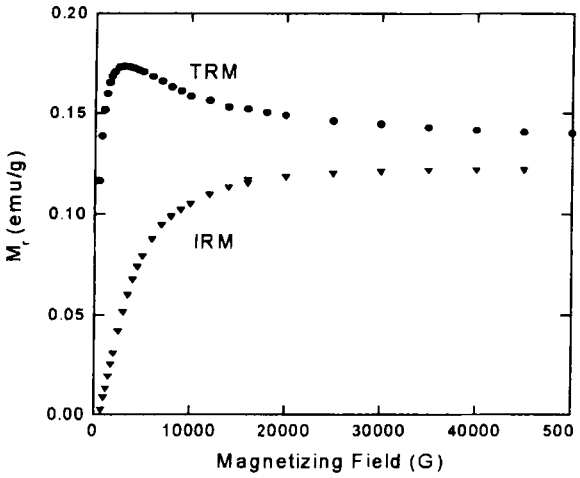

FIGURE 4 Isothermal remanent magnetization and thermal remanent magnetization data for the ferrite polymer composite plotted as a function of remanent inducing magnetic field.

quenched but the spins are still aligned in their frozen state and the sample possesses a resultant moment. Hence, the TRM experiment displays a large remanence compared to the IRM, where the spins are aligned in a random fashion during the transition to the spin glass state since there is no external magnetic field to influence their alignment.

The TRM and IRM measurements are very sensitive to temperature. These measurements provide the most accurate estimation of the blocking temperature, T_B. The remanence obtained by TRM is greatly amplified at low temperatures, and the IRM displays a very minor dependence on temperature. The TRM rapidly decreases as the temperature is increased. The TRM and IRM curves eventually coincide and the remanence goes to zero. The point at which the TRM and IRM measurements coincide gives a very precise estimate of the blocking temperature, which in this case turns out to be 27.0 K.

The unusual magnetic properties of frustrated magnetic materials (*e.g.*, superparamagnets and spin glasses) make them excellent candidates for an experiment in which radiation is used to generate magnetic bubbles and holes on the surface of a material.[1] The most spectacular demonstration of the photoinduced magnetic effect appears on the TRM or IRM relaxation, $MR_{(t)}$, of frustrated magnetic materials at temperatures below the blocking temperature. A process for generating magnetic bubbles in the superparamagnetic nanoparticle composites involves cooling the superparamagnetic material to a specified temperature, which is well below the spin blocking temperature (T_B=27K) under zero applied magnetic field (H=0kG). This results in the freezing of a random orientation of the spins in the superparamagnetic material. The magnetic field of 1kG is then applied to the frozen superparamagnet. Because of the nature of the superparamagnetic state, the magnetization will show a slight increase to a value represented by the zero- field cooled magnetic susceptibility

data. While the field is applied to the frozen superparamagnet, the sample is exposed to the radiation supplied by the high pressure xenon lamp about 5s illumination time. The radiation is of sufficient intensity to cause local disruption of the spin blocked state and a realignment of the spins to the direction the applied magnetic field. The result of this radiation will be the generation of a magnetic moment within the domain walls determined by the boundary of the pulse. The effect of this experiment on the magnetization is to cause an increase in the remanent magnetic moment of the sample.

A plot of the SQUID magnetometer output as a function of time before, during and after the frozen superparamagnet is exposed to the radiation is illustrated in Figure 5. Following the pulse, there is initially a drop in the moment and then an

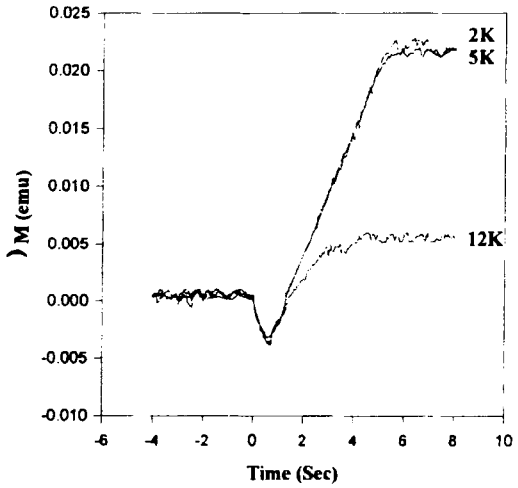

FIGURE 5 The magnetometer output for the photomagnetic response of the ferrite polymer composite plotted as a function of time before, during, and after a pulse of radiation.

increase in the magnetization to a new steady-state value that is substantially larger than the magnetization before the pulse. The initial drop in magnetic response is due to radiational heating of the sample. Indeed, the process of photomagnetic spin realignment may be a result of thermal effects; a thermal melting of the spins allows magnetic realignment. A slightly different phenomenon appears to occur in the material $Rb_{0.73}Cr_5Te_8$.

$\underline{Rb_{0.73}Cr_5Te_8}$

The crystalline material $Rb_{0.73}Cr_5Te_8$ is a new channel type structure prepared) from the elements at 850'C. It crystallizes 'in the monoclinic space group C2/m with cell dimensions a=18.539(3)A, b=3.9313(7)A, c=13.176(3)A and β=129.80(1)deg. The structure is based upon the Hollandite structure, and consists of $CrTe_2$ layers connected by $CrTe_6$ face and edge sharing octahedral, resulting in the formation of channels along the b direction. Spaces in these layers are subsequently filled BV rubidium. This structure differs from those structures already determined for the

family ACr_5X_8 (A=alkali metal, X=S, Se, Te), in the mode of connection between the layers. A schematic of the $Rb_{0.73}Cr_5Te_8$ structure is shown in Figure 6.[15] The short

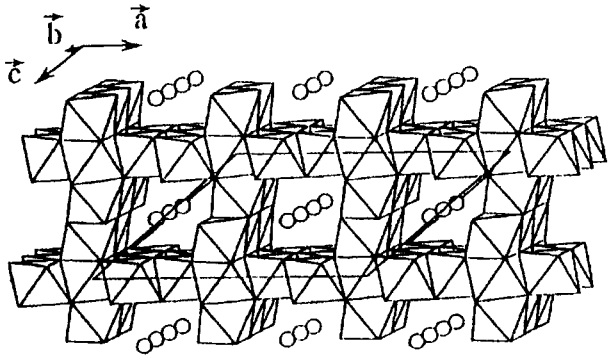

FIGURE 6 A diagram that illustrates the structure of the pseudo Hollandite $Rb^{0.73}$ Cr^5 Te^8.

Cr-Cr distances are restricted to two chromium atoms only with a slightly Longer distance of 3.153A. The chain of three chromium atoms is isolated with respect to the stacking direction. with the parallel chains being separated by a regular Cr-Cr distance of 3.931A. As a result of this complex bonding structure, the magnetic exchange of this material also shows a complicated behavior resulting in frustration and "spin glass" like properties.

Figure 7 illustrates temperature dependence of magnetic susceptibility of $Rb_{0.73}Cr_5Te_8$ for field cooled and zero field cooled experiments at low temperature.

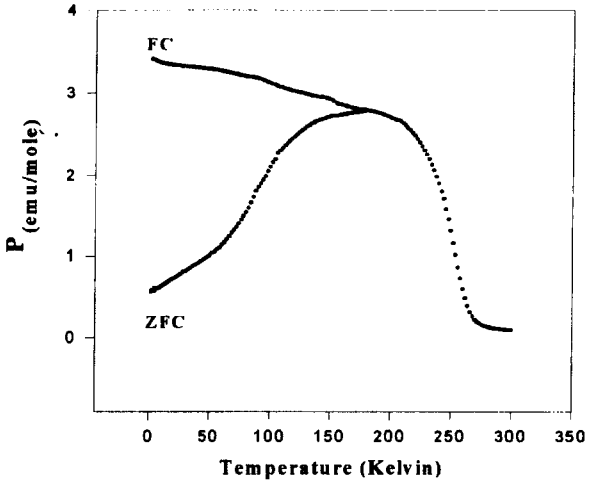

FIGURE 7 Field cooled (FC) and zero field cooled (ZFC) dc magnetic susceptibility data for $Rb_{0.73}$ Cr_5Te_8 plotted over the 1.7 to 300K temperature region.

The maximum that is observed in the zero field cooled magnetic susceptibility data and absent in the field cooled ones is a strong evidence that the $Rb_{0.73}Cr_5Te_8$ exists in a spin glass state with a freezing temperature of about 175K.

The analysis of the field dependence of the isothermal remanent magnetization (IRM) and thermal remanent magnetization (TRM) on $Rb_{0.73}Cr_5Te_8$ show that the TRM has a larger remanent magnetization relative to the IRM. A hump in the TRM curve has been observed and is characteristic of the spin glass state. Both IRM and TRM data curves converge to the same saturation remanent magnetization at higher magnetic fields reflecting the destruction of the spin glass state.

The same process for generating magnetic bubbles in a spin glass material of $Rb_{0.73}Cr_5Te_8$ was used. A plot of the SQUID magnetometer output at several temperatures recorded as a function of time before, during and after the frozen spin glass is exposed to the radiation is illustrated in Figure 8. Following the pulse, there is

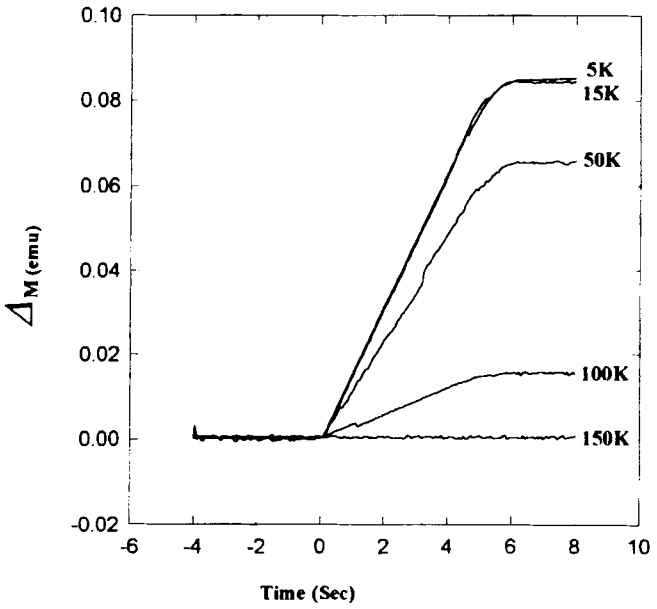

FIGURE 8 The magnetometer output for the photomagnetic response of $Rb^{0.73}$ Cr^5 Te^8 plotted as a function of time before, during, and after a pulse of radiation. The experiment is plotted at several temperatures.

an increase in the magnetization to a new steady-state value that is substantially larger than the magnetization before the pulse. The magnitude of the increase in magnetic response is directly correlated with the temperature of the sample. There is no apparent heating effect in this sample, probably because the magnetic effects occur over much larger temperatures than the previous example. Also, it is evident that the pulse of radiation does not contain sufficient energy to raise the temperature of a cooled sample in a helium bath to the spin blocking temperature of 175K. The photomagnetic effect must therefore result from an absorption of radiation and a

concomitant electronic transition, resulting in an unblocking of the spin and realignment of the spin with the magnetic field.

CONCLUSION

Two different types of frustrated magnetic systems are magnetically analyzed and both show photomagnetic behavior. The nanoferrite/polymer composite exhibits superparamagnetic behavior with a spin blocking temperature of 27K and a photomagnetic effect when irradiated at temperatures below the spin blocking temperature. The $Rb_{0.73}Cr_5Te_8$ analog is a non-stoichiometric solid that exhibits spin glass behavior with a relatively high freezing temperature of 175K. The material shows a strong photomagnetic effect at all temperatures below the spin glass freezing temperature. The photomagnetic effect in $Rb_{0.73}Cr_5Te_8$ results from absorption of radiation that producing an electronic transition and an uncoupling of the spins from the frozen spin glass alignment.

ACKNOWLEDGMENT

CJO wishes to acknowledge support from the Army Research Office grant administered by Battelle, grant #TCN96-137.

REFERENCES

1. C. J. O'Connor, The Photomagnetic and Magneto-Optic Effects, in Localized and Itinerant Magnetic Materials: From Molecular Assemblies to the Devices, E. Coronado, F. Palacio, D. Gatteschi, and J. S. Miller, Eds., Kluwer Academic Publishers, Dordrecht, The Netherlands (1996), in press.
2. C. J. O'Connor, E. Sinn, T.J. Bucelot, and B.S.Deaver, Chem. Phys. Lett., 74, 27, (1980)
3. S. Decurtins, P. Gütlich, K. M. Hasselbach, A. Hauser, and H. Spierling, Inorg. Chem., 24, 2174, (1985); P. Gütlich and A. Hauser, Coord. Chem. Rev., 97, 1 (1990); P. Gütlich, A. Hauser, and H. Spiering, Angew. Chem. Intl. Ed. Engl., 33, 2024, (1994); and references therein.
4. O. Kahn, J. Krober, and Charlotte Jay, Advanced Materials, 4, 718, (1992)
5. J. S. Philo, Proc. Natl. Acad. Sci. USA, 74, 2620, (1977).
6. O. Sato, T. Toyoda, A. Fujishima, K. Hashimoto, Science, 272, 704, (1996).
7. C. J. O'Connor and J. F. Noonan, J. Phys. Chem. Solids, 48, 303-307, (1987).
8. M. Ayadi and J. Ferré, J. Magn. Magn. Mags., 91, 54-57, (1986); M. Ayadi and J. Ferré, International Conference on Magnetism (at Franciso, 1985, Abstract # 4Pc16); M. Ayadi and J. Ferré, Phys. Rev. Lett. 50, 274, (1983); M. Ayadi and J. Ferré, J. Appl. Phys., 55, 1720, (1984); M. Ayadi and J. Ferré, Phys. Rev., 44, 10079, (1991).

9. J. -S. Jung, B. Wu, L. Ren, J. Tang, J. Ferré. J. Jamet, C. J. O'Connor, J. Appl. Phys., 73, 5463, (1993).
10. S.S. Dindun and E.A. Raitman, Sov. Phys.Solid State, 20 , 1108, (1978); K. Kovalenko and I.I. Kondilenko, Sov. Phys. JETP, 47, 386, (1978).
11. C. Petit, P. Lixon, M.P. Pileni, J Phys Chem, 94, 1598, (1990).
12. E.C. O'Sullivan, R.M. Patel, A.J.I. Ward, J Colloid Interface Sci, 146, 582, (1991).
13. S. Mann, J. Hannington, J Colloid Interface Sci, 122, 326, (1988).
S. Bhandarkar, A. Bose, J Colloid Interface Sci, 139, 541, (1990).
14. N.S. Kommareddi, M. Tata, V.T. John, G.L. McPherson, M.F. Herman, Y.S. Lee, C.J. O'Connor, J.A. Akkara and D.L. Kaplan, Chem. Mater, 8, 801-809, (1996).
15. J. Gareth, F. Boucher, M. Evain, C. J. O'Connor, and S. Li, J. Solid State Chem, 122, 41-45, 1996 and references therein.
16. C. J. O'Connor, Prog. Inorg. Chem, 29, 203-283, (1982).
17. M.A. Lopez-Quintela, J. Rivas, J Colloid Interface Sci, 158, 446, (1993).
18. M. Fuller, W.S. Goree, W.L. Goodman, Magnetite Biomineralization and Magnetoreception in Organisms, Kirschvink, J.L., Jones, D.S., MacFadden, B.J., Eds.; Plenum Press: New York, 103, (1985).
19. B.D. Cullity, Introduction to Magnetic Materials, Addison-Wesley: Reading, MA, 94, (1972).
20. I.I. Yaacob, A.C. Nunes, A. Bose, D.O. Shah, J Colloid Interface Sci, 171, 73, (1995).
21. R.F. Zoilo, E.P. Giannelis, A.B. Weinstein, M.P. O'Horo, B.N. Ganguly, V. Mehrotra, M.W. Russell, D.R. Huffman, Science, 257, 219, (1992).
22. R. Kaiser, G. Miskolczy, J Appl Phys, 41, 1064, (1970)
23. J.H. Zhang, T.L. Birdwhistell, C.J. O'Connor, Solid State Commun, 74, 443, (1994).
C.J. O'Connor, Research Frontiers in Magnetochemistry, O'Connor, C.J., Ed.; World Scientific Publishing, Inc.: London, 109, (1993).
24. D. Fiorani, Studies of Magnetic Properties of Fine Particles and Their Relevance to Materials Science, Dormann, J.L., Fiorani, D., Eds.; Elsevier: Lausanne, 135, (1992).
25. M.E. McHenry, S.A. Majetich, J.O. Artman, M. DeGraef, S.W. Staley, Phys Rev B, 49, 11358, (1994).
E.M. Brunsman, R. Sutton, E. Bortz, S. Kirkpartick, K. Midelfort, J. Williams, P. Smith, M.E. Mchenry, SEA. Majetich, J.O. Artman, M. DeGraef, S.W. Staley, J Appl Phys, 75, 5882, (1994).